The HKU Scholars Hub   The University of Hong Kong   香港大學學術庫

Title	Experimental and numerical investigation of post-tensioned concrete flat slabs in fire
Author(s)	Wei, Y; Au, FTK; Li, J; Tsang, NCM
Citation	The 8th International Conference on Structures in Fire (SiF'2014), Shanghai, China, 11-13 June 2014. In Progress on Safety of Structures in Fire: Proceedings of the 8th International Conference on Structures in Fire, 2014, v. 1, p. 229-238
Issued Date	2014
URL	http://hdl.handle.net/10722/204679
Rights	This work is licensed under a Creative Commons Attribution-NonCommercial-NoDerivatives 4.0 International License.

Experimental and Numerical Investigation of Post-tensioned Concrete Flat Slabs in Fire

Ya Wei [1], Francis T. K. Au [2], Jing Li [3] and Neil. C. M. Tsang [4]

1. Department of Civil Engineering, The University of Hong Kong, Hong Kong, China. E-mail: weiya@connect.hku.hk

2. Department of Civil Engineering, The University of Hong Kong, Hong Kong, China. E-mail: francis.au@hku.hk

3. Department of Civil Engineering, South China University of Technology, Guangzhou, China. E-mail: scutlijing@126.com

4. Department of Civil Engineering, Architecture and Building, Coventry University, UK. E-mail: aa8607@coventry.ac.uk

Abstract: Four tests of post-tensioned high-strength self-compacting concrete flat slabs were conducted under fire conditions. Tendon distributions of the slabs including the Distributed-Distributed and Banded-Distributed patterns as well as various loading ratios were considered. Two of the specimens with lower moisture contents demonstrated excellent fire resistance performance, while the others with slightly higher moisture contents experienced severe concrete spalling. The test results are presented and discussed in respect of thermal profiles, deflections, crack patterns and concrete spalling. Moreover, numerical modelling employing the commercial package ABAQUS was conducted to help interpret the test results in order to get better understanding of such slabs in fire.

Keywords: Concrete spalling; Fire; High-strength self-compacting concrete; Post-tensioned flat slab

Deleted: temperature distributions

1. INTRODUCTION

Post-tensioned (PT) concrete flat slabs with unbonded tendons have been increasingly adopted in both commercial and residential buildings for floor systems all over the world with the remarkable merits of reduced span-to-depth ratio and enhanced load-carrying capacity. Nevertheless, the fire resistance design requirements for flat slabs presented in the codes ACI 318-08 [1] and BS EN 1994-1-2 [2] and the professional manual [3] based on limited research results obtained decades ago are mainly prescriptive. Improved understanding of the true behaviour of flat slabs under fire conditions will therefore be helpful to better fire resistance design in consideration of structural safety and cost.

The pioneering research on PT concrete flat slabs exposed to ASTM E119 standard fire has been reported by Gustaferro [4], where no concrete spalling occurred and the fire resistance periods exceeded 3 hours. From the studies, recommendations of minimum concrete cover and critical temperature of prestressing steel tendons were proposed for required fire resistance periods. However, as pointed out by Gales *et al.* [5], these tests could be out of date with respect to construction material and technique employed, and quite insufficient for performance-based fire resistance design. Nevertheless, few fire tests of PT concrete flat slabs have been carried out since then, except for the fire tests of one-way PT concrete slabs conducted in the recent decade mainly in Mainland China and the UK. Yuan *et al.* [6] have investigated the effects of sequential fire exposure on continuous unbonded PT concrete slabs, namely exposing the middle span to fire for 90 minutes and then the end span to fire for 90 minutes in succession, or in reverse. It was concluded from the investigation that the damage modes of the slabs were significantly

2

affected by the sequence of fire exposure. Zheng *et al.* [7] have tested simply-supported PT concrete slabs and two-span PT concrete slabs with the two spans exposed to fire simultaneously, where specimens were cast with normal strength concrete with calcareous coarse aggregate. The strength ranged from 40 MPa to 60 MPa and the moisture contents from 2.36% to 3.98% by mass. In the experiments, concrete spalling was observed, and an envelope diagram was proposed with respect to normal stress, concrete strength and moisture content for preliminary judgment of possibility of concrete spalling. In the UK, Bailey and Ellobody [8] conducted fire tests of simply-supported PT concrete slabs with unbonded tendons at the same time, taking into consideration the aggregate types and longitudinal restraints. The results showed that the structural behaviour was dominated by the thermal expansion of aggregate, and that longitudinal restraints could reduce the slab deflection because of arching action formed in the slab due to the restraining force.

Previous tests have provided better understanding of the performance of one-way PT normal-strength concrete slabs under fire conditions. Further investigation is therefore necessary to understand the structural fire performance of two-way PT flat slabs, particularly their deformations and load-carrying mechanisms in fire. Moreover, high-strength self-compacting concrete (HSSCC) is becoming increasingly popular in modern building construction, but it is sensitive to concrete spalling when exposed to fire due to its relatively low permeability and lower porosity [9,10]. Therefore, the present investigation is to explore the behaviour of PT HSSCC flat slabs with unbonded tendons in fire based on experimental and numerical approaches.

2. **TESTS AND NUMERICAL MODELLING**

2.1. **General**

The test specimens, denoted as Test-1, Test-2, Test-3 and Test-4, respectively, were identical in geometry but different in tendon arrangement and loading ratio, as shown in Table 1. The tendon arrangement in each direction were banded or distributed. The design prestressing level was specified by the ratio of the final average PT tendon stress to the ultimate strength. The design loading ratio was that of the applied loads including the self-weight of slab to the ultimate loading capacity of the slab.

Figure 1 shows one of the test specimens, which comprises a flat slab supported on four columns seated on a base grid of beams. Only the central panel of the slab enclosed by the columns was exposed to fire, while the rest of slab and columns were protected from fire with ceramic wool. The numerical model of one quarter of the specimen shown in Figure 2 was established employing the ABAQUS package. The concrete and prestressing tendons were modelled by three-dimensional (3D) solid elements while the steel reinforcing bars were modelled by 3D truss elements. Frictionless contact between the prestressing tendons and the surrounding concrete was assumed in the model. The thermal and mechanical properties of the materials at elevated temperature and the thermal parameters for convection and radiation were taken from BS EN 1991-1-2 [11] and BS EN 1992-1-2 [2], respectively. The concrete used for the slab and columns in the tests was grade C60 HSSCC with granite aggregate and ground granulated blast-furnace slag (GGBS), with composition given in Table 2. Grade C40 normal concrete was used for the support beams.

4

2.2. **Specimens**

The specimens were designed according to BS EN 1992-1-1 [12] and ACI 318 [1] to reduced scale due to the dimensional limitation of the furnace. Figure 3 shows the details of dimensions and reinforcement of the specimens. The slab is square in plan with sides of 3.1 m and depth of 95 mm. The columns have square cross sections of 200 mm by 200 mm with a clear height from the top of base to the soffit of slab of 1850 mm. The base beams have a breadth of 200 mm and depth of 400 mm, and have lengths of 2600 mm and 1800 mm in X and Y directions respectively. Besides, top and bottom steel reinforcing bars of the slab were mild steel round bars of grade 235 and 6 mm diameter provided with concrete cover of 15 mm. High yield steel deformed bars of grade 335 and 12 mm diameter were provided to the columns and base beams as longitudinal reinforcement, while mild steel round bars of grade 235 and 6 mm diameter were used as stirrups. The concrete cover to the reinforcement in columns and base beams was 25 mm.

Figure 4 shows the tendon arrangement for two specimens. Figure 4(a) shows the Distributed-Distributed tendon arrangement, where tendons in the X direction denoted as X1 to X6 adopt the profile "Tendon-profile-a1" while tendons in the Y direction denoted as Y1, Y2, Y5 and Y6 adopt the profile "Tendon-profile-a2" and those denoted as Y3 and Y4 adopt the profile "Tendon-profile-a3". Figure 4(b) shows the Banded-Distributed tendon arrangement, where tendons in the X direction denoted as X1 to X6 adopt the profile "Tendon profile-b1" while tendons in the Y direction denoted as Y1 and Y6 adopt profile "Tendon profile-b2" and those denoted as Y2 to Y5 adopt profile "Tendon profile-b3"

5

The mild steel round bars of grade 235 had measured properties of elastic modulus of 190 GPa, yield strength of 248 MPa and ultimate strength of 410 MPa, while the corresponding measured properties of high yield steel deformed bars of grade 335 were 196 GPa, 458 MPa and 582 MPa, respectively. The strand has a nominal diameter of 12.7 mm and cross sectional area of 98.7 mm^2, which is greased and housed in a polypropylene sleeve with thickness of 1 mm. In view of the reduced scale, the minimum concrete cover to the tendons was 21.5 mm. The measured mechanical properties of strand at ambient temperature included elastic modulus of 211GPa, 0.2% proof stress of 1805 MPa and ultimate strength of 2008 MPa.

2.3. **Instrumentation**

The deflections of slabs were measured by Linear Variable Displacement Transducers (LVDTs) denoted as VD-1 to VD-6 in Figure 3. LVDTs VD-1 and VD-2 were used to monitor the vertical displacements of the central panel at the loading points; VD-3 and VD-5 were used to monitor the vertical displacements at the middle of column strips in the X direction; and VD-4 and VD-6 were used to monitor the vertical displacements at the middle of column strips in the Y direction. Self-made and calibrated load cells were used to measure the tendon forces during tensioning. Thermocouples were placed in the specimen to measure the thermal profiles of slab as shown in Figure 4. Taking the middle of X3 as an example, X3-B, X3-S, X3-P, X3-M and X3-T denote the bottom, bottom reinforcement, tendons, middle and top of the slab respectively where the temperatures were measured by thermocouples.

6

Deleted: temperature distributions

2.4. **Test procedure**

The furnace used as shown in Figure 5(a) has a clear height of 1.8 m, clear width of 3.0 m and clear length of 4.0 m. The loading system is comprised of a hydraulic jack with a loading capacity of 500kN and simply-supported steel beams in contact with four steel load spreaders, as shown in Figure 5(b). Firstly, loads were applied on the slab through the loading system and were kept constant for 15 mins for stability. Afterwards, fire was started in the furnace for testing with the applied loads maintained. The fire curves monitored in the four tests are compared with the ISO 834 standard fire curve in Figure 6, which shows reasonable agreement.

Besides, the HSSCC strengths at 28 days and on the test day, average initial forces of tendons and those after loss, loads not including self-weight of the slabs, and moisture contents were recorded as shown in Table 3. The moisture content was determined from two concrete cores taken from each specimen by weighing both before and after heating in an oven at the temperature of 105℃ for 24 hours according to BS 476-20 [13].

3. **RESULTS AND DISCUSSIONS**

Results obtained from the tests are presented covering the thermal profiles, deflections, crack patterns and concrete spalling. These results are also discussed based on numerical modelling for better understanding the PT flat slabs in fire.

7

Deleted: with two concrete cores taken from each specimen by weighing both before and after heating in an oven at the temperature of 105℃ for 24 hours

Deleted: temperature distributions

3.1. Thermal profile

Figure 7 shows the variations of thermal profile in the slabs with time. While Figures 7(a) and 7(b) show relatively smooth temperature curves, Figures 7(c) and 7(d) appear irregular as a result of severe concrete spalling. As shown in Figures 7(a) and 7(b), the temperature of the slab soffit rose quickly after starting of fire due to heat transfer through radiation and convection. Obviously, with the increase of distance from the soffit, the temperature had a slower heating rate due to the relatively high thermal resistance of concrete. There are only slight differences between the temperatures measured at X3 and Y3 in Test-1, and Y3 and Y2 in Test-2 at the same level. However, in Test-1 the temperature of tendon X3 was much higher than that of Y3 as the concrete covers to them were 27.5 mm and 38.5 mm respectively. Therefore it can be concluded that the measured thermal profiles are reliable and reasonably accurate. Besides, Figures 7(a) and 7(b) show excellent agreement between the numerical results and test results, verifying that the thermal properties of materials and thermal parameters in the numerical model are reliable.

Interestingly, there are plateaus observed in the tendon temperatures in Figures 7(a), 7(b) and 7(c) in the range from about 130℃ to 160℃. This may be caused by the melting of polypropylene sleeves in conjunction with moisture evaporation, but it cannot be achieved by the present numerical modelling. In addition, the thermal profiles were severely affected by the continuous concrete spalling since 5 minutes after the test began. For example, the temperatures of the soffit and reinforcement increased dramatically at the temperature of 200℃ in Figure 7(c), and there is a temperature leap in Y2-B in Figure

7(d) due to thermal shock caused by concrete spalling. Besides, comparing the

temperatures of X3-P in Test-1 and X3-P in Test-3, the former is much lower than the latter, indicating that concrete spalling can accelerate the increase of tendon temperature.

The temperatures at the top surface of the central panel in the first two tests without concrete spalling are further examined. In Test-1, it reached 160°C after 75 minutes of fire exposure, and the fire was conservatively discontinued as the tendon temperature already exceeded the critical temperature of 350°C prescribed in BS EN 1992-1-2 [2]. In Test-2, it reached 240°C at 120 minutes after commencement. In accordance with the failure criteria in BS 476-20 [13] with respect to insulation, Test-1 did not violate the criteria but Test-2 did. Generally, Test-2 only had a fire resistance of 90 minutes according to the criteria, but it survived 120 minutes still with structural integrity and stability.

3.2. **Vertical displacements**

Figure 8 shows the vertical displacements of the slabs in Test-1 and Test-2. In the figure, VD-C is the average value of VD-1 and VD-2 denoting the vertical displacement of central panel; VD-X is the average of VD-3 and VD-5 denoting the vertical displacement of column strip in the X direction; and VD-Y is the average of VD-2 and VD-6 denoting the vertical displacement of column strip in the Y direction. The deflections of the slabs are mainly governed by the thermal gradients across the depth of the slabs and the consequent thermal expansions [14], as well as restraint-induced thermal thrust forces. Moreover, the mechanical properties of concrete, reinforcement and prestressing tendons

degraded and stress relaxation of tendons with the increase of temperature all resulted in the reduced stiffness of the slab and further contributed to the increase of deflections.

Figures 8(a) and 8(b) show that vertical displacements of the central panel increased rapidly in the initial 15 minutes. Afterwards, the increases of displacements gradually slowed down with time due to the reduced temperature gradient and increased thermal thrust forces due to restraints provided by the columns and the surrounding cold parts of slab. The vertical displacements of the column strips in the X direction and the Y direction also increased a lot in the first 15 minutes but they slowed down afterwards or even remained constant. The displacements are mainly caused by the flexural deformation of the central panel in the two orthogonal directions leading to the flexural deformation of the column strips. Moreover, VD-X is larger than VD-Y because the column strip span in the X direction is larger than that in the Y direction and hence the former has smaller flexural stiffness. Besides, as observed in Figure 8(b), after the initial 90 minutes, VD-C changed slightly faster, while VD-X and VD-Y had no obvious changes. This can be explained by the cracks that appeared in and parallel with the column strips. The cracks weakened the integrity of slab releasing the rotation restraints from the cold parts of slab, further leading to the increase of deflection in the central panel.

The predicted displacements obtained from numerical modelling show reasonable agreement with those obtained from Test-1 and Test-2, but obvious discrepancies still exist as shown in Figure 8. The discrepancies may be attributed to two aspects. One is that the thermal expansion of concrete considered in numerical modelling, which is taken

to be that of siliceous normal concrete from BS EN 1992-1-2 [2], while the concrete in the tests is HSSCC. The other aspect is that transient thermal creep strain of concrete was not explicitly considered. Further refinement is necessary.

3.3. **Crack distribution**

Figure 9(a) shows the crack distribution at the top surface of slab in Test-1 after fire. The cracks mainly appeared in the column strips adjacent to the cold parts of slab approximately in an elliptic pattern. As observed during the test, cracks first appeared in and parallel with column strips in the Y direction after the initial 25 minutes. Figure 9(b) shows the maximum principal stress distribution obtained from numerical modelling at that time. The maximum tensile stresses are mainly distributed in the column strips adjacent to the cold parts of slab, which is consistent with the crack distribution. Moreover, the tensile stresses are mainly caused by negative moments induced by the restraints of the adjacent cold parts of slab on the doubly curved deformation of the central panel. Interestingly, neither cracking nor spalling was observed at the soffit of the central panel as shown in Figure 9(c), because the in-plane concrete stresses at the soffit of slab were either slightly tensile or even compressive in two directions due to restrained thermal expansion.

Figure 10 shows that the cracks and tensile stress distributions of the slab in Test-2 are similar to those in Test-1, and the soffit shows neither cracking nor spalling. However, Test-2 survived more than 120 minutes of fire exposure, which resulted in more cracks at the top surface, as shown in Figure 10(a). Besides, the tensile stress distribution of the

slab is slightly different as stress concentration is slightly more significant in column strips in the X direction than that in the Y direction as shown in Figure 10(b) because of the additional tensile stress perpendicular to the banded prestressing tendons. The tensile stress distribution is consistent with the crack distribution, which further validates the numerical model.

The cracks mainly appeared around the boundary between the central panel and the surrounding cold parts of slab resulting in the release of restraints to the central panel. It suggests that the load-carrying capacity of the slab should be greatly reduced but it was not the case, as the deflection still developed steadily without collapse. Besides, the fact that the soffit of slab remained smooth implied that the expected flexural deformation based on yield line theory might not work. So one may deduce that tensile membrane action could have been present, enhancing the load-carrying mechanism of the slab. Moreover, it can be seen that tendon distribution has minor effects on the crack patterns, but its impact on the tensile stress distribution is relatively obvious.

3.4. **Concrete spalling**

Severe concrete spalling occurred to the slabs of Test-3 and Test-4, causing premature failure of the slabs by tendon fracture or spalling-induced through holes in slab. However, the numerical models used could not consider the reduction in slab section due to fragmentation and explosive spalling of concrete, which may cause discrepancies in prediction. The major factors affecting concrete spalling at elevated temperature include pore pressure due to moisture, thermal stress due to restraint against thermal expansion,

12

and their combined effects. However, the mechanism of concrete spalling still remains controversial.

In Test-3, a series of popping sounds were intermittently heard since 5 minutes after fire exposure and they continued for 25 minutes. Then several big "bangs" were heard as well. Afterwards, it remained more or less quiet, but after 35 minutes of fire exposure, a strong cracking sound was heard. After 40 minutes of fire exposure, a small area of concrete exploded at the top surface of slab near the load spreader, which is denoted as TS-1 (where TS stands for top spalling) in Figure 11(a). After 50 minutes of fire exposure, another relatively large area of concrete exploded also near the load spreader, which is denoted as TS-2, and the test was terminated. Finally no through hole was formed in the slab. At the end of 40 minutes of fire exposure, the water that appeared earlier on the top surface was evaporated completely, leaving behind the slab dry in appearance. It suggests that the explosive spalling is mainly caused by the thermal and compressive stresses in accordance with Hertz [15].

Detailed examination of the slab after fire revealed a large area of concrete at the soffit of slab having spalled as shown in Figure 11(b). Different degrees of spalling are observed, which are denoted as BS-1, BS-2 and BS-3 (where BS stands for bottom spalling). BS-1 is less severe with only concrete cover having spalled, while BS-2 and BS-3 are quite severe as the concrete above the bottom layer of reinforcement has spalled, where compressive stresses have been relatively large at commencement of fire as shown in Figure 11(c). Besides, one strand fractured due to direct exposure to fire. The overall

13

spalling is more than half of the soffit area, but it is not uniform possibly due to non-uniform moisture distribution.

In Test-4, similar sounds were heard as well. The differences are that the popping sounds were more intensive from the time after 10 minutes of fire exposure to the end, unlike those intermittent sounds in Test-3. In particular, near the end of test, significant explosive spalling happened forming a through hole in the slab with crushed concrete pieces flying upward violently. The spalled area and position are denoted as TS-1 in Figure 12(a). Just a few seconds later, similar explosive spalling denoted as TS-2 happened again, which was much stronger and much larger in area. Nevertheless, the slab did not collapse.

By examining the soffit of slab as shown in Figure 12(b), it can be found that nearly the whole area of soffit concrete has spalled except for a small part in the central panel. The violent spalling mainly occurred approximately at the quarter positions of the panel in the two directions, as the compressive stresses were distributed as shown in Figure 12(c). As the column supported corners were protected from fire, the most violent spalling therefore occurred at the quarter position that was reasonably close to the corner, under large compressive stresses and pore pressure in concrete, and just outside the perimeter of the top reinforcement layer. Obviously, the top reinforcement also played an important role in preventing through holes induced by spalling. Moreover, there was neither fracture of tendons nor reinforcing bars.

Test-1 and Test-3 have the same loading ratio, and their moisture contents are 2.27% and 2.62%, respectively. Test-2 and Test-4 have identical parameters, except that their moisture contents are 2.36% and 2.52%, respectively, but they have completely different results. Obviously, the moisture content is significant in accounting for the differences, and is the main factor regarding possible concrete spalling. More importantly, one may assume that there is a threshold moisture content between 2.36% and 2.53% that triggers concrete spalling under certain compressive stresses.

Besides, the degree of spalling in Test-3 is less severe compared with that in Test-4 because the compressive stresses at the soffit of the central panel as induced by the applied loads and post-tensioning in Test-3 were smaller than those of Test-4, even though the moisture content in Test-3 is slightly higher. It therefore indicates that compressive stress is another key factor governing possible concrete spalling. When the concrete was completely dried by heating, explosive concrete spalling still happened, suggesting that spalling was caused by compressive stresses as a result of restrained thermal expansion and flexural compression at the top surface of slab.

4. **CONCLUSIONS**

Among the four tests, two of the specimens with lower moisture contents demonstrated excellent fire resistance performance without concrete spalling. The other two specimens with higher moisture contents experienced severe concrete spalling leading to shorter fire resistance periods. The following conclusions can be drawn:

(a)   The tendon distribution has minor effect on the structural responses of the slabs. The deflections of slabs are dominated by temperature gradient and thermal expansion, as well as restraint-induced thrust forces. The crack distribution is mainly governed by the doubly curved deformation of slabs and the negative moments induced.

(b)   The cracks did not lead to the collapse of slab. Instead, they released some of the restraints to the doubly curved deformation of the central panel, which further contributed to the formation of tensile membrane action that enhanced the fire resistance of the slabs.

(c)   There may be a threshold moisture content that triggers concrete spalling under certain compressive stresses. In the tests, the threshold is between 2.36% and 2.53%.

(d)   Concrete spalling is mainly governed by moisture content and compressive stresses. After the concrete spalling is triggered, it develops in a progressive manner. However, with the progress of fire, the effect of moisture content gradually reduces while the effect of ensuing compressive stresses becomes more important.

ACKNOWLEDGEMENTS

References

1. ACI 318-08, Building code requirements for structural concrete (ACI 318-08) and commentary, ACI Standard, <u>American Concrete Institute</u>, Farmington Hills, Mich, USA, 2008.

2. BS EN 1992-1-2, Eurocode 2: design of concrete structures—part 1-2: general rules-structural fire design, <u>British Standards Institution</u>, London, UK, 2004.

3. PTI, Post-Tensioning Manual, sixth edition, <u>Post-Tensioning Institute</u>, Phoenix, AZ, 2006.

4. Gustaferro, A., Fire resistance of post-tensioned structures, <u>Journal of the Prestressed Concrete Institute</u>, 1973, 18(2), 38-63.

5. Gales, J. Bisby, L. and Gillie, M., Unbonded post tensioned concrete in fire: A review of data from furnace tests and real fires, <u>Fire Safety Journal</u>, 2011, 46(4), 151-163.

6. Yuan, A. Dong, Y. and Gao, L., Behavior of unbonded prestressed continuous concrete slabs with the middle and edge span subjected to fire in sequence, <u>Fire Safety Journal</u>, 2013, 56, 20-29.

7. Zheng, W. Hou, M. Shi, D. and Xu, M., Experimental study on concrete spalling in prestressed slabs subjected to fire, <u>Fire Safety Journal</u>, 2010, 45(5), 283-297.

8. Bailey, C. and Ellobody, E., Fire tests on unbonded post-tensioned one-way concrete slabs, <u>Magazine of Concrete Research</u>, 2009, 61(1), 67-76.

9. Noumowe, A. Carre, H. Daoud, A. and Toutanji, H., High-strength self-compacting concrete exposed to fire test, <u>Journal of Materials in Civil Engineering</u>, 2006, 18(6), 754-758.

10. Anagnostopoulos, N. Sideris, K. and Georgiadis, A., Mechanical characteristics of self-compacting concretes with different filler materials, exposed to elevated temperatures, <u>Materials and Structures</u>, 2009, 42(10), 1393-1405.

11. BS EN 1991-1-2, Eurocode 1: Actions on structures – Part 1-2: General actions – Actions on structures exposed to fire, <u>British Standards Institution</u>, London, UK, 2002.

12. BS EN 1992-1-1. Eurocode 2: Design of concrete structures – Part 1-1: General rules and rules for buildings, <u>British Standards Institution</u>, London, UK, 2004.

13. BS 476-20, Fire tests on building materials and structures – Part 20: Method for determination of fire resistance of elements of construction (general principles), <u>British Standards Institution</u>, London, UK, 1998.

14. Usmani, A. Rotter, J. Lamont, S. Sanad, A. and Gillie, M., Fundamental principles of structural behaviour under thermal effects, <u>Fire Safety Journal</u>, 2001, 36(8), 721-744.

15. Hertz, K., Limits of spalling of fire-exposed concrete, <u>Fire Safety Journal</u>, 2003, 38(2), 103-116.

Table 1: Parameters investigated in the tests

Test Case	Tendon distribution	Design prestressing level	Design loading ratio
Test-1	Distributed-Distributed	0.37	0.50
Test-2	Banded-Distributed	0.50	0.35
Test-3	Distributed-Distributed	0.50	0.50
Test-4	Banded-Distributed	0.50	0.35

Table 2: High-strength self-compacting concrete mixture (kg/m^3)

Cement	GGBS	Fine aggregate	Coarse aggregate	Water	Additives
394	106	650	1060	142	11.65

Table 3: Concrete strength, tendon forces, applied loads and moisture content for the tests

Test Case	Concrete strength (MPa)		Forces of tendons (kN)		Loads (kN)	Moisture content
	28 Days	Day of test	Initial	After loss		
Test-1		76.6	98.4	72.4	85.7	2.27%
Test-2	78.9	75.6	119.7	95.4	85.7	2.36%
Test-3		79.5	127.3	94.8	125.7	2.62%
Test-4		81.4	123	91.5	85.7	2.52%

Figure 1: Overview of one test specimen
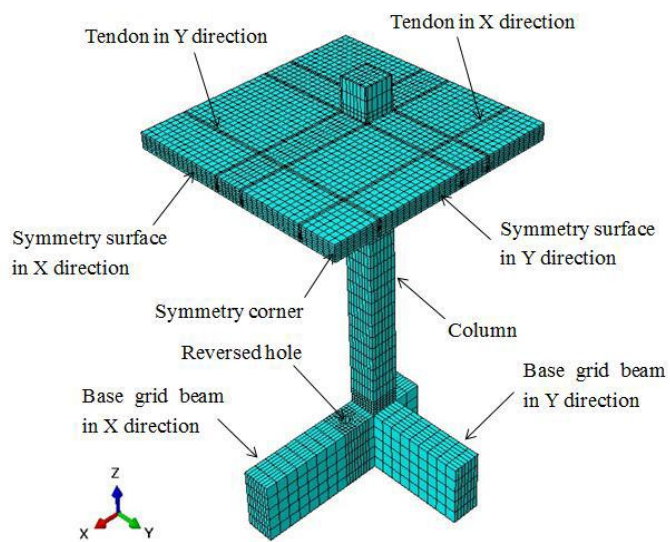
Figure 2: Numerical model of a quarter of specimen
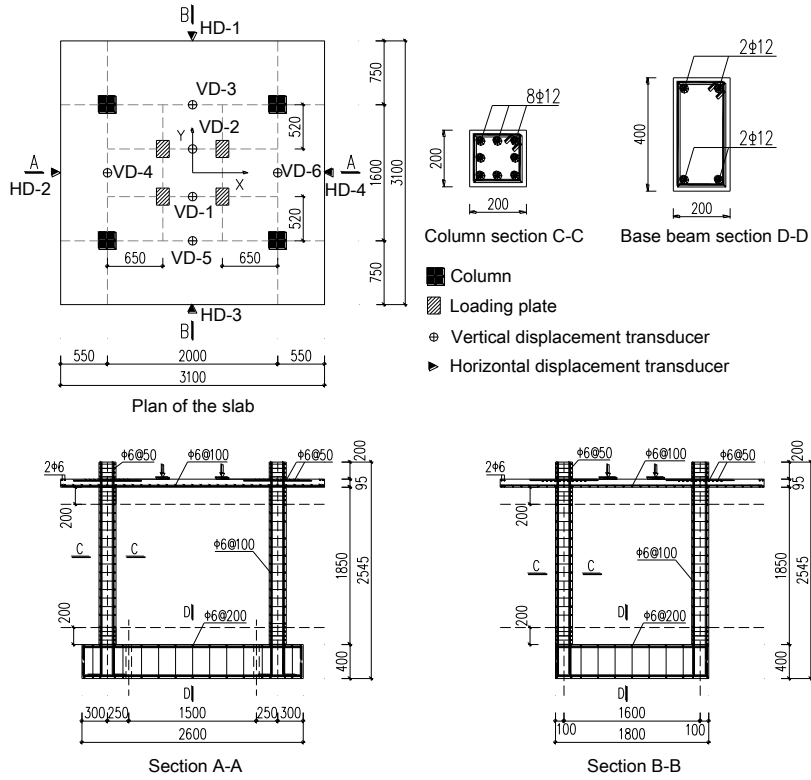
Figure 3: Configuration of test specimens and arrangement of loading and displacement transducers (dimensions in mm)
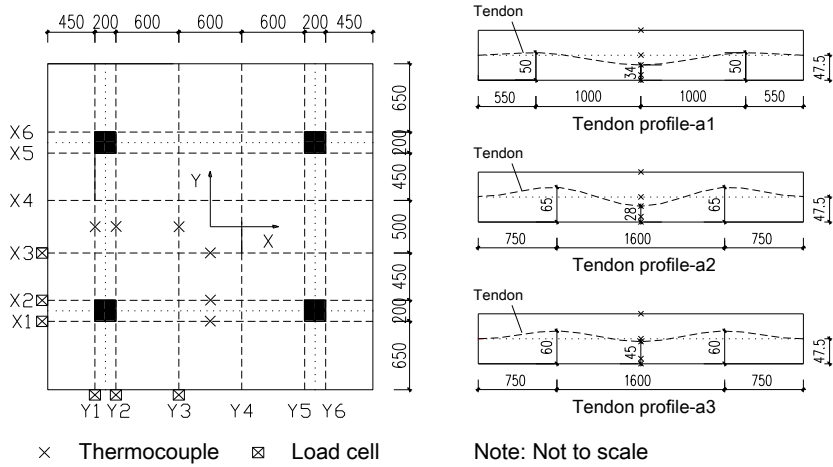
(a) Distributed-Distributed
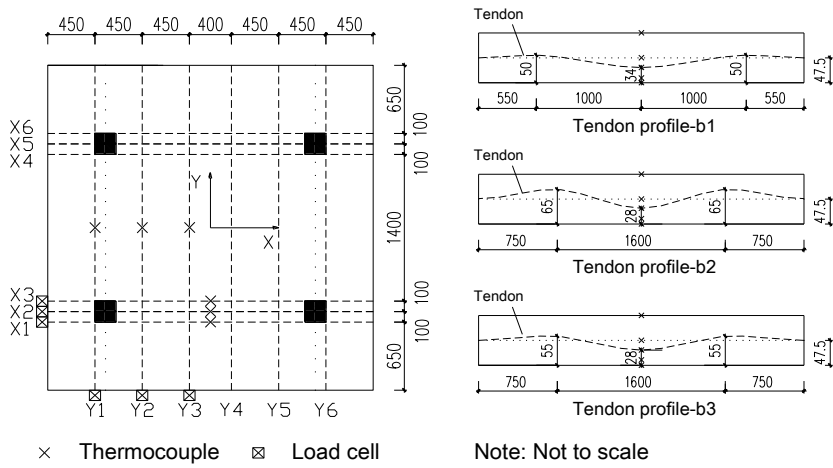
(b) Banded-Distributed

Figure 4: Arrangement of tendons and thermocouples (dimensions in mm)

22

(a) Furnace

(b) Loading system

Figure 5: Test furnace and loading system
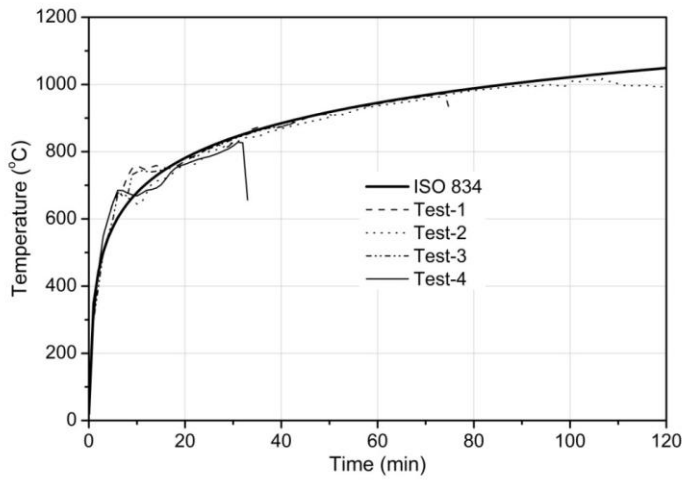
Figure 6: Furnace fire curves and standard fire curve
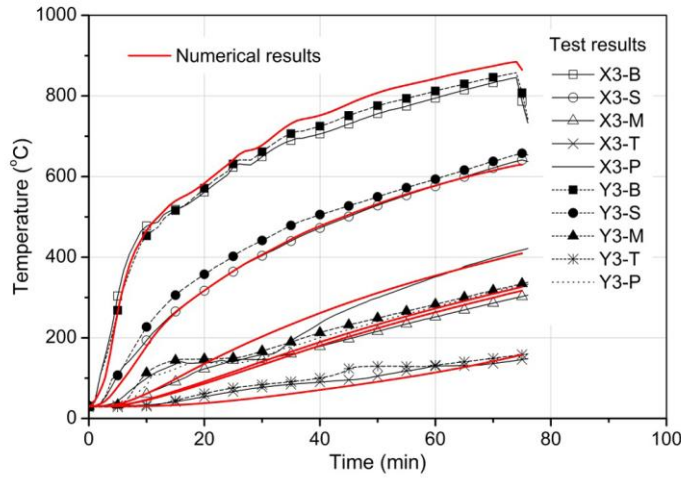
(a) Test-1
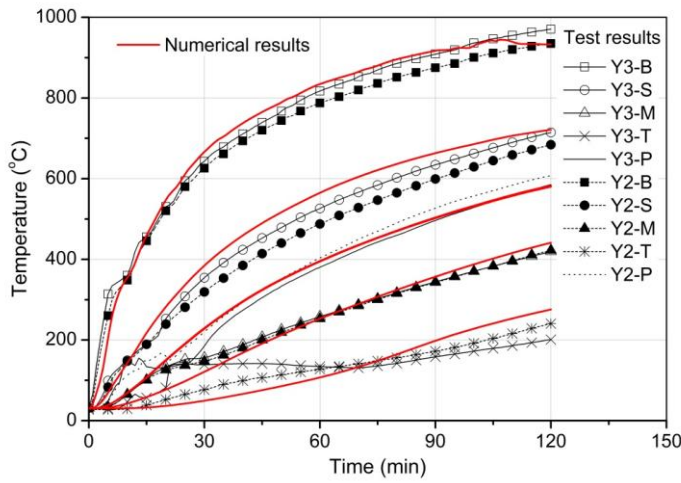
(b) Test-2

Figure 7: Temperature variations of central panel of slab
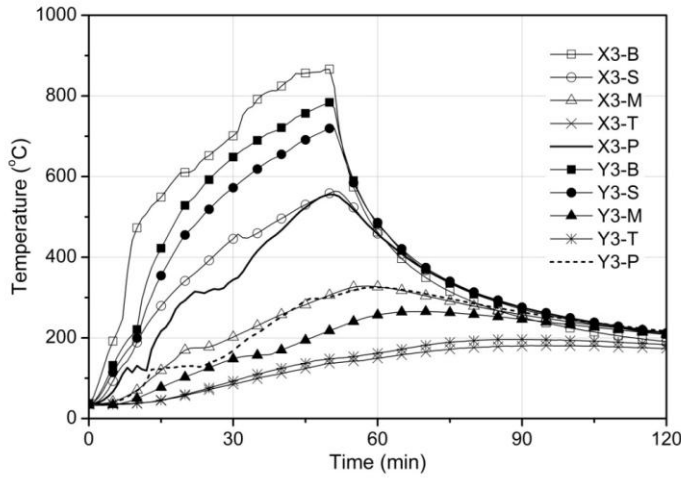
(c) Test-3
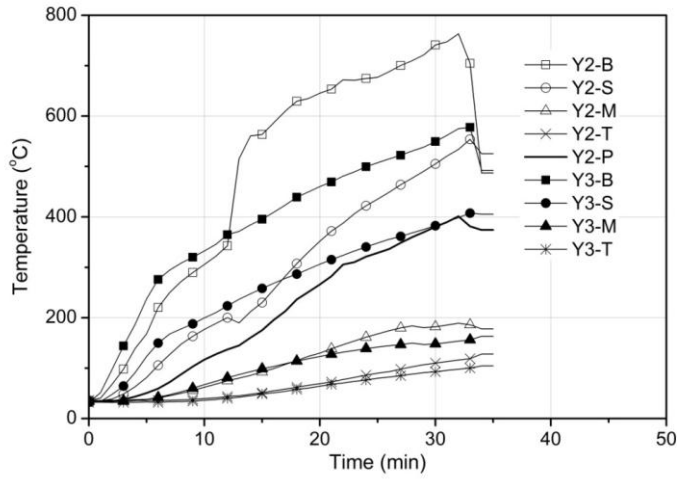
(d) Test-4

Figure 7: Temperature variations of central panel of slab (continued)
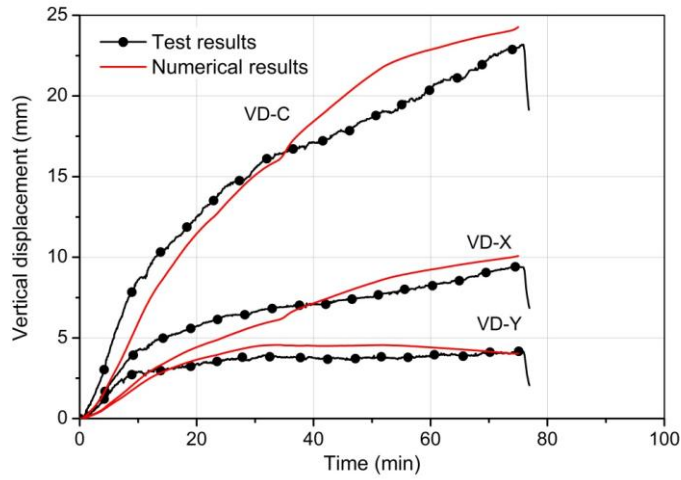
(a) Test-1
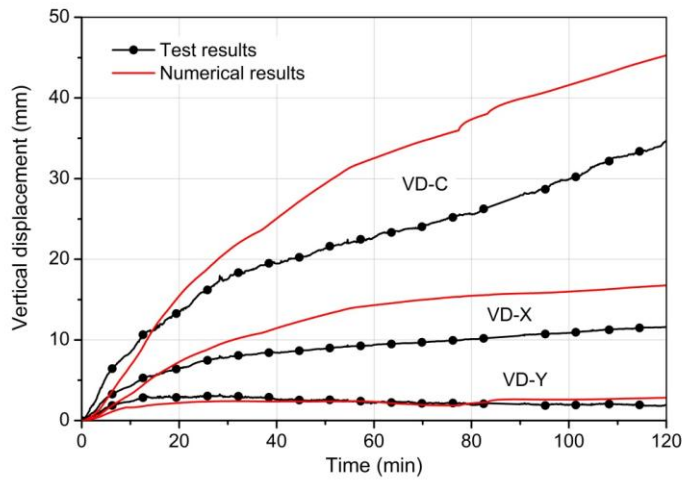
(b) Test-2

Figure 8: Vertical displacements of slabs
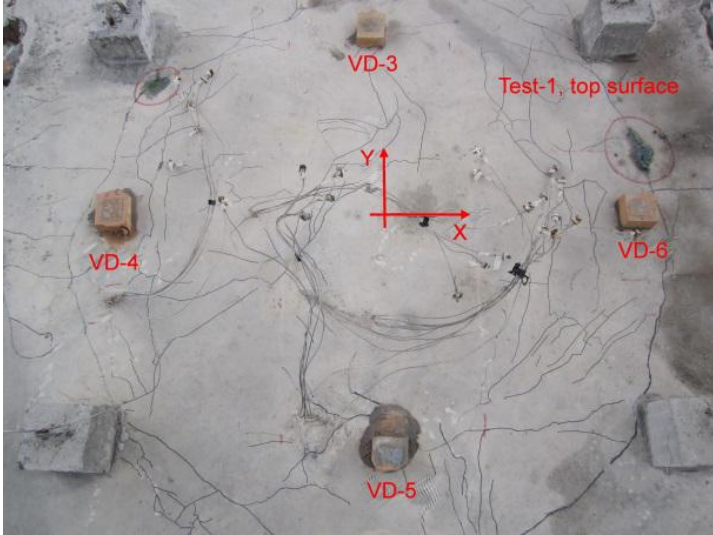
(a) Cracks at top surface after fire
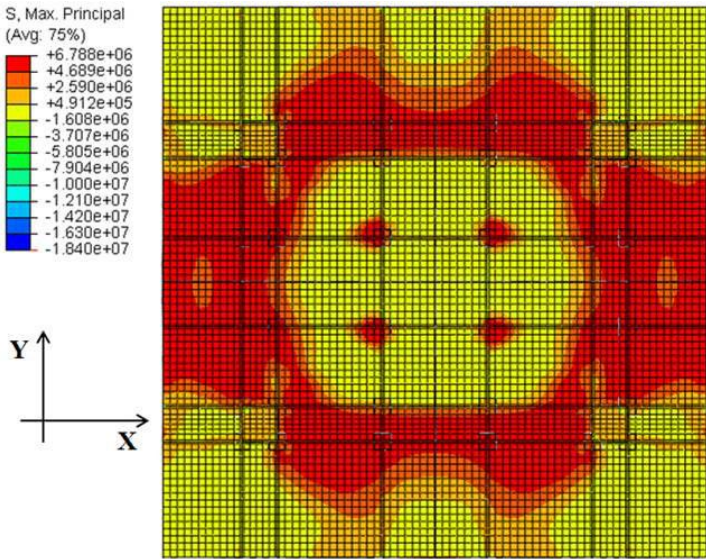
(b) Stress distribution at top surface at 25 min in fire

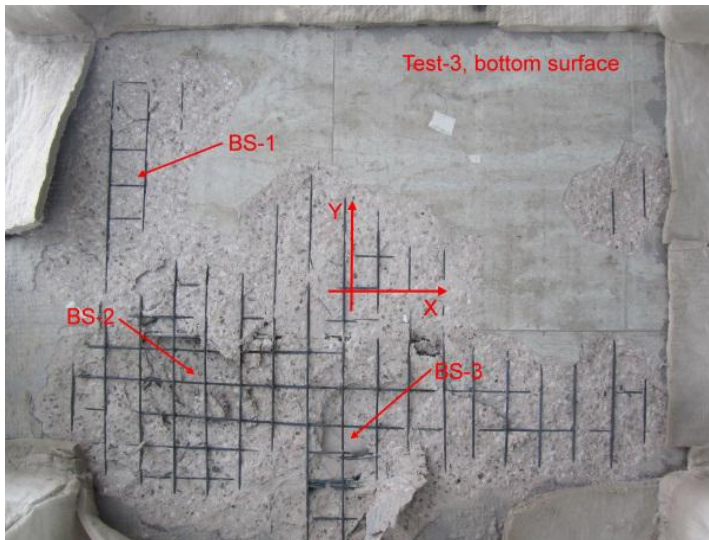Figure 9: Cracks and stress distribution of the slab in Test-1

28
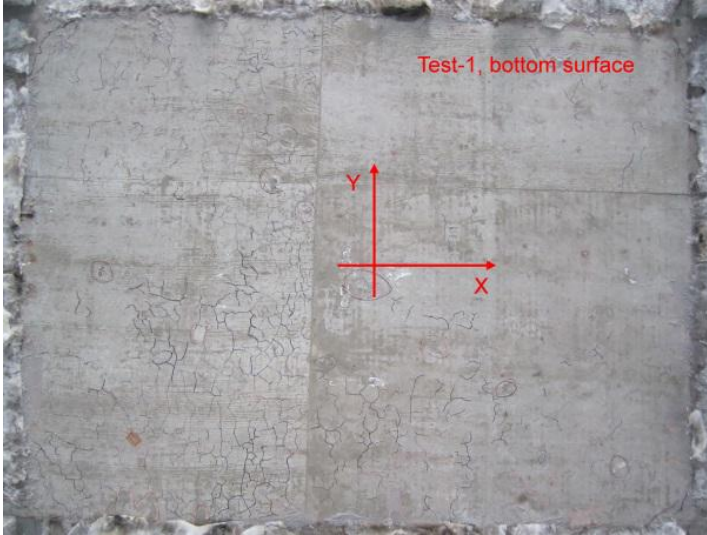
(c) Cracks at soffit after fire

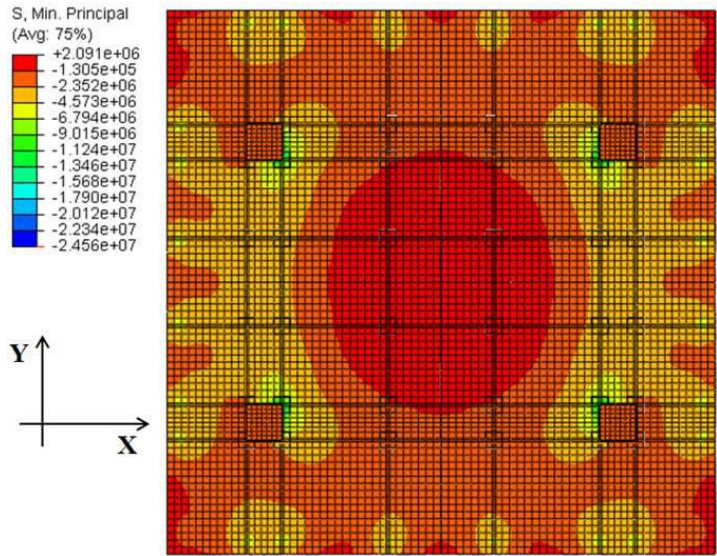Figure 9: Cracks and stress distribution of the slab in Test-1 (continued)
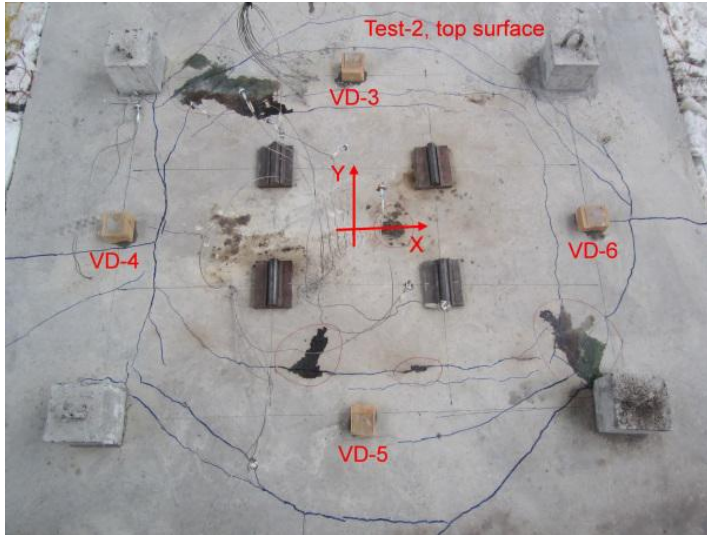
(a) Cracks at top surface after fire
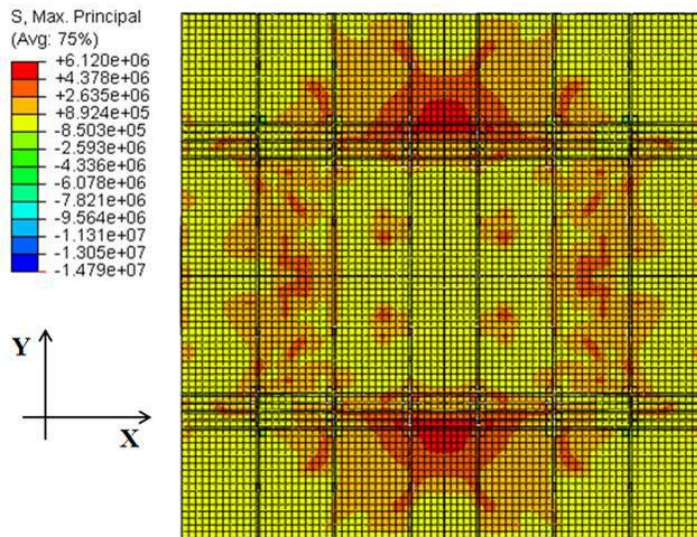
(b) Stress distribution at top surface at 25 min in fire

Figure 10: Cracks and stress distribution of the slab in Test-2
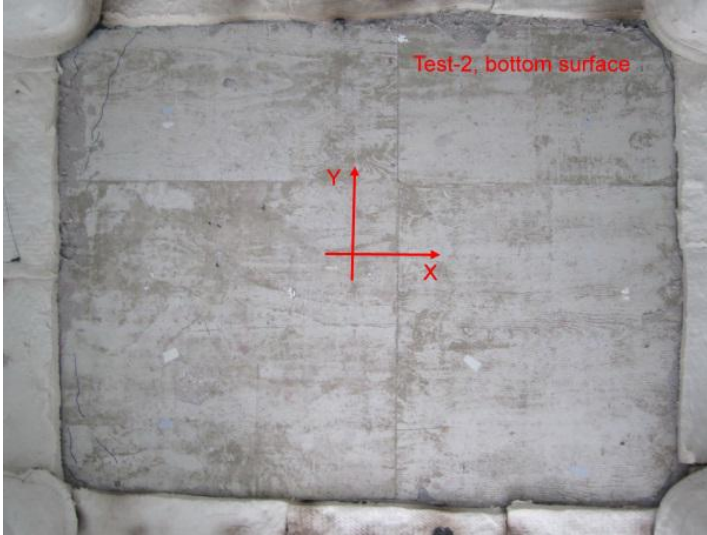
(c) Cracks at soffit after fire

Figure 10: Cracks and stress distribution of the slab in Test-2 (continued)
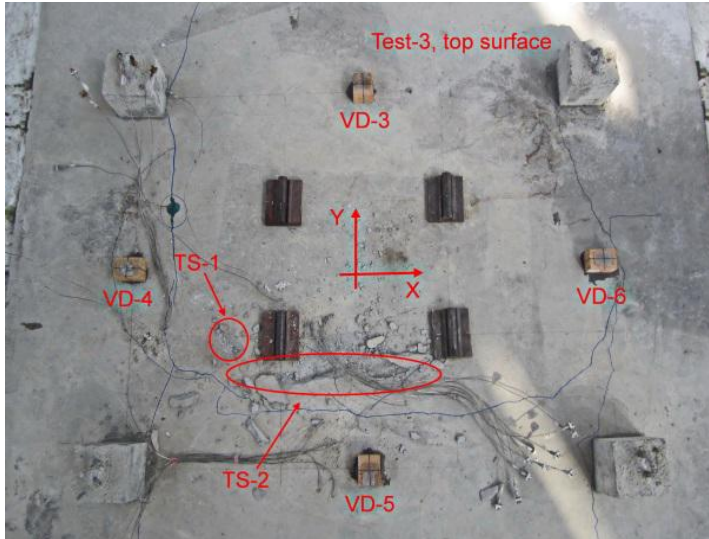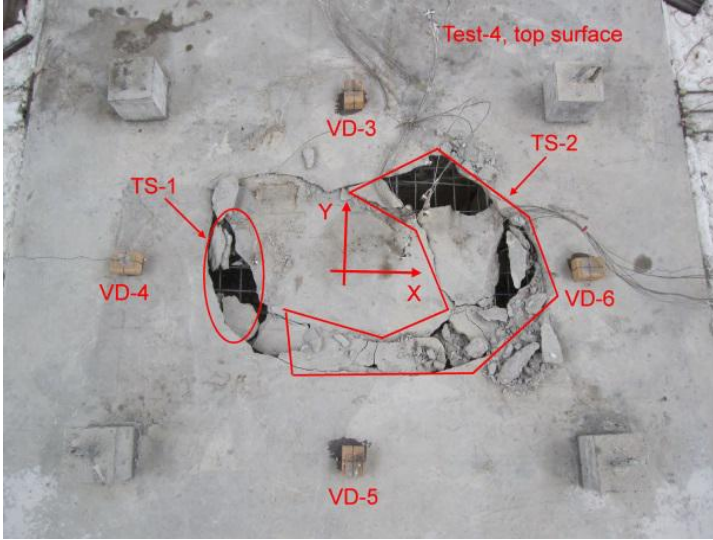
(a) Top surface spalling

(b) Soffit spalling

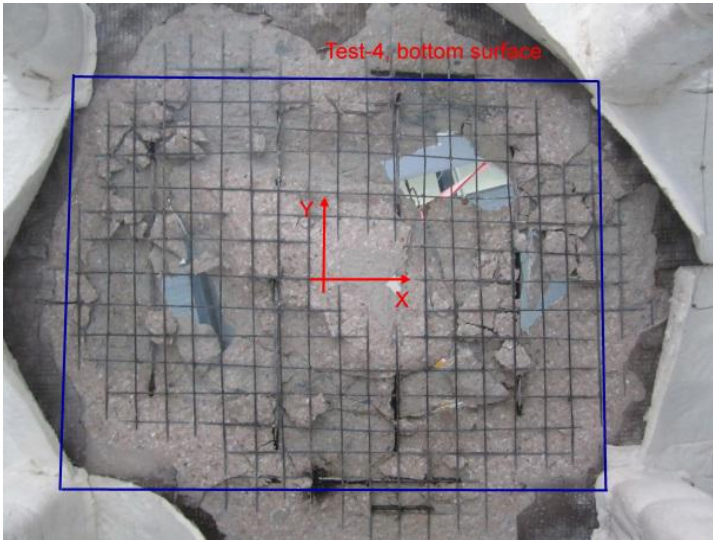Figure 11: Concrete spalling and stress distribution of the slab in Test-3

(c) Compressive stress distribution at soffit at commencement of fire

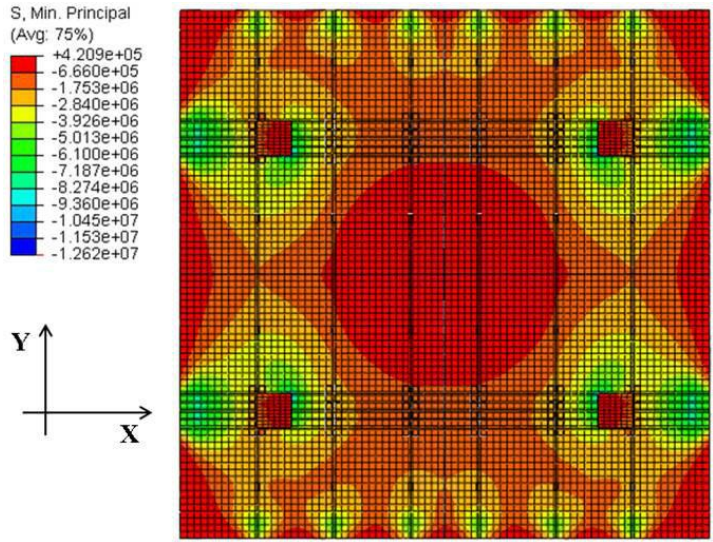Figure 11: Concrete spalling and stress distribution of the slab in Test-3 (continued)

(a) Top surface spalling

(b) Soffit spalling

Figure 12: Concrete spalling and stress distribution of the slab in Test-4

(c)

Figure 12: Concrete spalling and stress distribution of the slab in Test-4 (continued)